Zuse Institute Berlin

Takustraße 7
D-14195 Berlin-Dahlem
Germany

SEBASTIAN GÖTSCHEL, CHRISTIAN HÖHNE,
SANJEEVAREDDY KOLKOORI, STEFFEN MITZSCHERLING,
JENS PRAGER, MARTIN WEISER

Ray Tracing Boundary Value Problems: Simulation and SAFT Reconstruction for Ultrasonic Testing

ZIB Report 16-14 (March 2016)

Zuse Institute Berlin
Takustraße 7
D-14195 Berlin-Dahlem

Telefon: 030-84185-0
Telefax: 030-84185-125

e-mail: bibliothek@zib.de
URL: http://www.zib.de

ZIB-Report (Print) ISSN 1438-0064
ZIB-Report (Internet) ISSN 2192-7782

Ray Tracing Boundary Value Problems: Simulation and SAFT Reconstruction for Ultrasonic Testing

Sebastian Götschel* Christian Höhne† Sanjeevareddy Kolkoori†
Steffen Mitzscherling† Jens Prager† Martin Weiser*

March 23, 2016

Abstract

The application of advanced imaging techniques for the ultrasonic inspection of inhomogeneous anisotropic materials like austenitic and dissimilar welds requires information about acoustic wave propagation through the material, in particular travel times between two points in the material. Forward ray tracing is a popular approach to determine traveling paths and arrival times but is ill suited for inverse problems since a large number of rays have to be computed in order to arrive at prescribed end points.

In this contribution we discuss boundary value problems for acoustic rays, where the ray path between two given points is determined by solving the eikonal equation. The implementation of such a two point boundary value ray tracer for sound field simulations through an austenitic weld is described and its efficiency as well as the obtained results are compared to those of a forward ray tracer. The results are validated by comparison with experimental results and commercially available UT simulation tools.

As an application, we discuss an implementation of the method for SAFT (Synthetic Aperture Focusing Technique) reconstruction. The ray tracer calculates the required travel time through the anisotropic columnar grain structure of the austenitic weld. There, the formulation of ray tracing as a boundary value problem allows a straightforward derivation of the ray path from a given transducer position to any pixel in the reconstruction area and reduces the computational cost considerably.

Introduction

Ultrasonic testing of inhomogeneous anisotropic materials, e.g., austenitic welds, has been a subject of increasing interest in recent years [1-6]. A main difficulty in the application of ultrasonic inspection techniques to anisotropic materials lies in the fact that in such materials sound velocity and refraction index depend on the phase direction of an incident wave, and phase direction and direction of energy propagation are no longer identical. This can lead to effects like beam

*Zuse Institute Berlin, Berlin, Germany
†BAM Bundesanstalt für Materialforschung und -prüfung, Berlin, Germany

skewing, beam splitting, or focusing and defocusing of sound fields [7, 8]. Inhomogeneous anisotropic media might consist of several homogeneous layers of different anisotropic materials or, as is the case for austenitic welds [7], be a structure with continuously varying anisotropic properties. In the latter case, ultrasonic waves will no longer propagate in a straight line or even piecewise straight trajectory, but along a curved path with varying sound velocity. Taking the aforementioned effects into account is necessary when evaluating data acquired by ultrasonic inspections of such materials.

The approach to use acoustic ray tracing to obtain information about inhomogeneous anisotropic structures, namely austenitic welds, was mainly developed in the 1980s. Basically, the comparison of simulated and measured travel times between a transducer and a receiver is used for fitting a parametric model of anisotropies or material defects. Since then, a variety of publications deal with different aspects of the method. One feature common to most of the work is the use of forward propagation of rays, mathematically speaking as initial value problems for ordinary differential equations. As the ray paths and hence their end points are not known in advance, many rays have to be computed in order to cover all receiver positions.

Here, we consider the formulation of the ray tracing problem as a two point boundary value problem as is common in isotropic seismic inversion [9, 10]. As both start and end point of the rays are prescribed, comparatively few boundary value problems need to be solved.

1 Boundary Value Ray Tracing in Layered Media

1.1 Mathematical Model

In inhomogeneous anisotropic media, the ray tracing ordinary differential equations (ODEs) are given as

$$\begin{aligned}\frac{dx_i}{d\tau} &= a_{ijkl}\, p_l\, g_j^{(m)}\, g_k^{(m)} \\ \frac{dp_i}{d\tau} &= -\frac{1}{2}\frac{\partial a_{jkln}}{\partial x_i}\, p_k\, p_n\, g_j^{(m)}\, g_l^{(m)}.\end{aligned}$$

Here, a_{ijkl} are the density-normalized elastic parameters, x is a 3D-position in Cartesian coordinates, τ denotes the travel time of the wave under consideration, and $p = \nabla\tau$ is called slowness vector. The eigenvalues of the Christoffel matrix $\Gamma_{ik} = a_{ijkl}\, p_j\, p_l$ are denoted by $g^{(m)}, m = 1, 2, 3$. Throughout the paper we use the Einstein summation convention for brevity.

For many applications it is of special interest to find one specific ray, connecting a sender and receiver with known positions x_S, x_R, such that the initial slowness vector p_0 is to be determined. Mathematically, this is a two-point boundary value problem consisting of the ray tracing system above, together with boundary conditions

$$r(y(0), y(T)) = \begin{pmatrix} x(0) - x_S \\ x(T) - x_R, \end{pmatrix}$$

where $y = (x, p)^\mathsf{T}$. The unknown time T when the ray reaches the receiver can be handeled by transforming the system to a fixed time interval $s \in [0, 1]$ instead of $\tau \in [0, T]$ and adding one equation for the constant final time T. For the required seventh boundary condition in this formulation we choose to prescribe an initial magnitude of the slowness vector, assuming the sender to be in an isotropic material with speed of sound v.

In layered structures, like dissimilar welds, the elastic parameters a_{ijkl} are discontinuous at the material boundaries. When the ray arrives at such an interface, refraction occurs, such that the slowness vectors of transmitted and reflected waves have to be computed. Refraction into an isotropic medium can be easily handled by computing

$$\tilde{p} = p - \left[p^\mathsf{T} n \pm \left(\tilde{v}^{-2} + v^{-2} + (p^\mathsf{T} n)^2 \right)^{1/2} \right] n,$$

where the interface normal n is oriented against the incident wave, and $\tilde{p}, \tilde{v}$ denote the refracted slowness vector and wave speed of the generated refracted wave. The plus sign corresponds to the transmitted wave, the minus sign gives the reflected wave. The relation holds for any wave type (compressional or shear). For refraction into an anisotropic medium the computations are more involved and require the solution of an algebraic equation of sixth order. We do not repeat the details here but refer to the literature, e.g., [11, 12].

The formulation as an ODE-boundary value problem allows to incorporate continuously varying elastic parameters without the need for an artificial discretization of the weld into layers or cells.

1.2 Solution Method

The solution of such systems can be computed numerically using shooting or collocation methods [13]. The simple single shooting aims at finding an initial value such that the corresponding solution of the initial value problem satisfies the terminal boundary conditions. This is done by finding a zero of the—in general nonlinear—boundary condition using Newton's method. The required derivatives can either be computed using the variational equations derived from the initial value problem [14], or with finite differences. As this information is required for amplitude computations as well, the computational overhead for the shooting method is small.

1.3 Numerical Results

For testing the proposed method, as well as for SAFT reconstruction in Section 2, we consider a specimen consisting of ferritic steel with an attached buffer, joined by a dissimilar weld to a component of austenitic steel. On top of the object, a perspex layer is added to account for the perspex wedge of the transducers used in the experiments. To describe the crystal orientation in the weld, we use the Ogilvy model [15], see Figure 1 for a sketch. For the isotropic base materials, longitudinal sound velocities of 5619 m/s for austenitic and 5935 m/s for ferritic steel were used. In the perspex zone, the sound velocity was set to

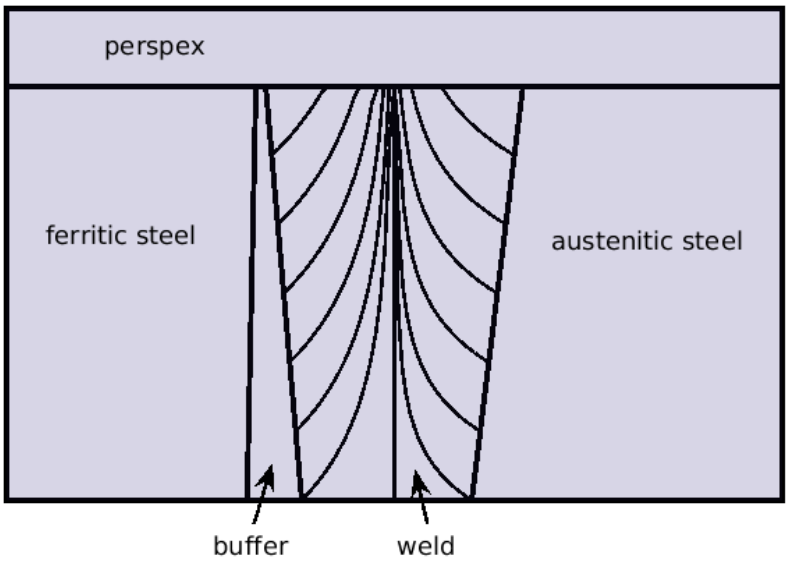

Figure 1: Sketch of the considered geometry. The height of the weld is 32 mm with an additional 6 mm perspex layer. The buffer has a layback angle of 11° and a constant crystal orientation of 82°, the weld has a layback angle of 8° and the crystal orientation given by the Ogilvy model with parameters $T = (-0.5614, 0.9266)$, $a = (5.6574, 3.9685)$, $\eta = 1$. The extension of the weld is 9.945 mm at the top and (5.9825 mm, 7.17 mm) at the bottom, right and left of the weld center. The x-coordinates of the buffer are 10.7 mm left of the weld center at the top, and 11.39 mm at the bottom.

2730 m/s. The elastic constants of weld and buffer material are (in GPa) given as $C_{11} = 247.25$, $C_{12} = 91.75$. $C_{13} = 133$, $C_{33} = 206$, $C_{44} = 119$, $C_{66} = 77.75$, with density 7980 kg/m^3. More details can be found in [6].

For the ODE formulation of the boundary value ray tracing, we use the continuously varying crystal orientations directly. As a comparison, we also consider a layer model, where the weld is discretized into layers of constant grain orientation. In Figure 2, we exemplarily show five rays computed with the continuous ODE model and the layer model in a cross section of the weld. Small differences are visible inside the weld, as expected. Two of the plotted rays differ already inside the isotropic region and the buffer, which is due so slightly differing paths in y-direction (along the weld, not plotted here). In Figure 3, the $L^2(0, T; \mathbb{R}^3)$-norm of the difference of the $x(\tau)$-component (position) between the continuous ODE solution and its approximation by the layered structure model with increasing number of layers. With about 25 layers, the accuracy of the layer model matches the prescribed tolerances of the ODE solver, with an

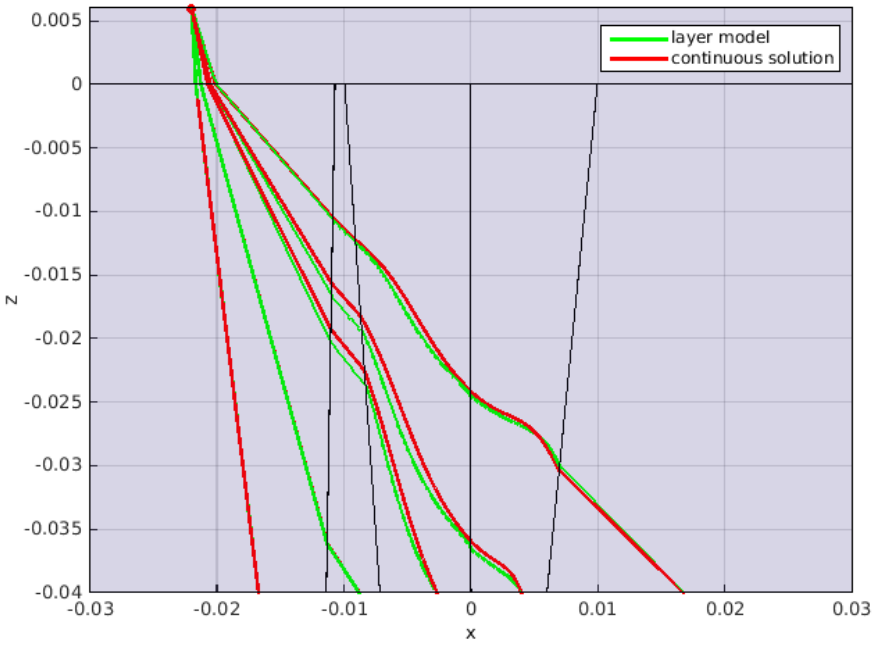

Figure 2: Comparison of boundary value ray tracing using a layer model (green) and a continuous model for the for the grain orientation (red) along a cross section of the specimen. As expected, small differences between the layer model and the ODE solution are visible inside the weld.

average 0.1 mm deviation between $x(\tau)$ of continuous and layer model.

The computational cost of boundary value ray tracing is considerably higher than for initial value problems, as it involves derivative computations and a Newton iteration to satisfy the boundary conditions. Computing the required Jacobian matrix for the seven components of the ray tracing system involves the computation of 49 additional rays. However, as soon as not only the time of flight is of interest, but the amplitudes at a receiver position, this matrix is needed anyway. Thus, the computational overhead is determined by the number of required Newton steps. This number strongly depends on the initial guess for the ray, and, in our numerical experiments, varied between five and 40, where the prescribed accuracy for finding a zero of the boundary condition was a distance of 1 μm. If not single rays are to be computed, but a scan of some region of interest (given by some set of receiver positions), the average number of Newton steps can be reduced by using the last computed ray as an initial guess for solving the boundary value problem for the next receiver position. For example, scanning along the z-axis for fixed (x, y)-coordinates of a receiver, the average number of Newton iterations was reduced from 21.7 to 2.3 per z-coordinate, with one Newton iteration taking on average 1.3 s. For scans along the x- and y-axis similar reductions in iteration counts were obtained.

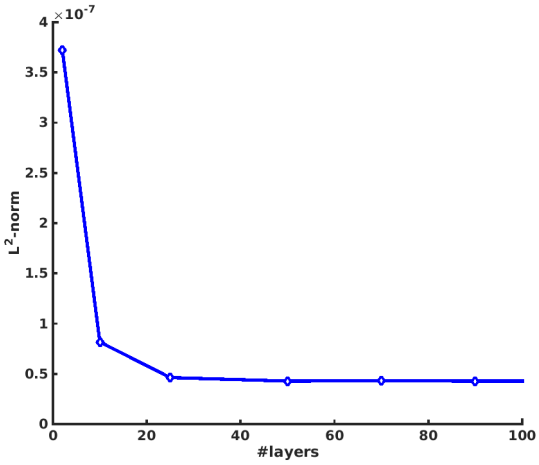

Figure 3: L^2-norm of the difference between continuous solution of the boundary value problem and its approximation by the layer mode with increasing number of layers for the second from right ray in Figure 2.

2 Combination with SAFT

2.1 SAFT

The synthetic aperture focusing technique (SAFT) is an imaging technique used in ultrasonic inspection. It allows a straightforward interpretation of measured data and offers a higher detectability of flaws compared with B-scan images by improving the SNR [16]. The basic idea is to move the transducer over the surface and take pulse echo measurements (A-scans) from different positions along the path. The region of interest is discretized into a grid of cells where all cells are initialized with a value of 0. For a given cell the times of flight to the different transducers at sender and receiver positions is calculated and the corresponding amplitudes found at these times in the respective A-scans are added to the cell value. If a reflector is present within a cell, the signals will add up constructively, increasing the amplitude. Otherwise, they will be added with a random phase shift, canceling each other on average. Repeating this procedure for all cells within the region of interest will lead to an image of the flaws in that region. Details of the algorithm can be found, e.g., in [17].

Calculating the times of flight between a defined transducer position and a particular cell within an inhomogeneous anisotropic structure is a nontrivial task and requires modeling of the sound field propagation through the structure by ray tracing or other means. A detailed description of the use of forward ray tracing in combination with SAFT (RT-SAFT) for the imaging of transverse cracks in austenitic and dissimilar welds can be found in [6]. The basic idea of RT-SAFT with forward ray tracing is to define a ray bundle emanating from the source point, trace each ray individually, calculate the times of flight along the ray paths and store them in a look up array for each cell the ray passes through.

This look up array can then be used to determine the times of flight relative to each transducer position from which measurements were taken as long as the inhomogeneous anisotropic structure can be assumed to be invariant in scan direction (which is the case for weld inspections with scans along the weld run direction). When modeling the ray bundle, a sufficient number of rays has to be chosen to ensure that every cell within the region of interest is hit at least once. This means that cells close to the source point will be hit by a large number of rays while at a greater distance single cells might be missed entirely if focusing effects occur within the inhomogeneous anisotropic structure.

With the use of a two point boundary value ray tracer instead of simple forward modeling, we can specify start and end point of each ray. This allows us to ensure that the look up array is fully populated, i.e. the time of flight is calculated for each cell within the region of interest. Preventing gaps in the look up array ensures that all data taken from measurements that are relevant to the region of interest will be processed during the SAFT reconstruction which should have a positive impact on the quality of the SAFT image by avoiding needless loss of information about the region of interest. Furthermore, by choosing the endpoints of each ray appropriately, we can ensure that the times of flight are calculated between the source point and the exact center of the cell that is to be evaluated. Compared to taking the time of flight at a more or less random point within the cell through which a forward modeled ray passes, this allows for a more accurate SAFT reconstruction in the sense that phase shifts due to errors in times of flight are minimized, thus further enhancing the quality of the obtained image.

Additionally, an adaptive strategy for populating the travel time matrix is easily implemented. In a first step, the weld is discretized using large cells, such that only comparatively few rays have to be computed. These travel times can then be used in a SAFT reconstruction to determine a smaller region of interest. In this area, better approximations of the times of flight can be obtained using a finer discretization and a second ray tracing step for the new cells. As the previously computed neighboring rays can be used as a good initial guess, only very few Newton iterations will be required.

2.2 Results and Discussion

To verify the boundary value ray tracing approach it is compared to the initial value ray tracing. Therefore, a specimen that contains an artificial flaw (notch, 6 mm depth) was scanned via impulse-echo technique. The measured signal values are allocated to the volume cells as explained in section 2.1 resulting in the SAFT reconstructions shown in Figure 4.

The reconstruction of a notch results in two spots where the summed signals gain local amplitude maxima: One at the base of the notch and one at its tip. Both models reconstruct the flaw in the correct depth (26 mm to 32 mm). For the boundary value ray tracing, the mapping of the flaw is better and the microstructure of the weld (e.g. grains) is better defined, while the initial value ray tracing produces a more diffuse reconstruction. The reason can be found in the calculation of the travel times: A ray that hits the center of each cell

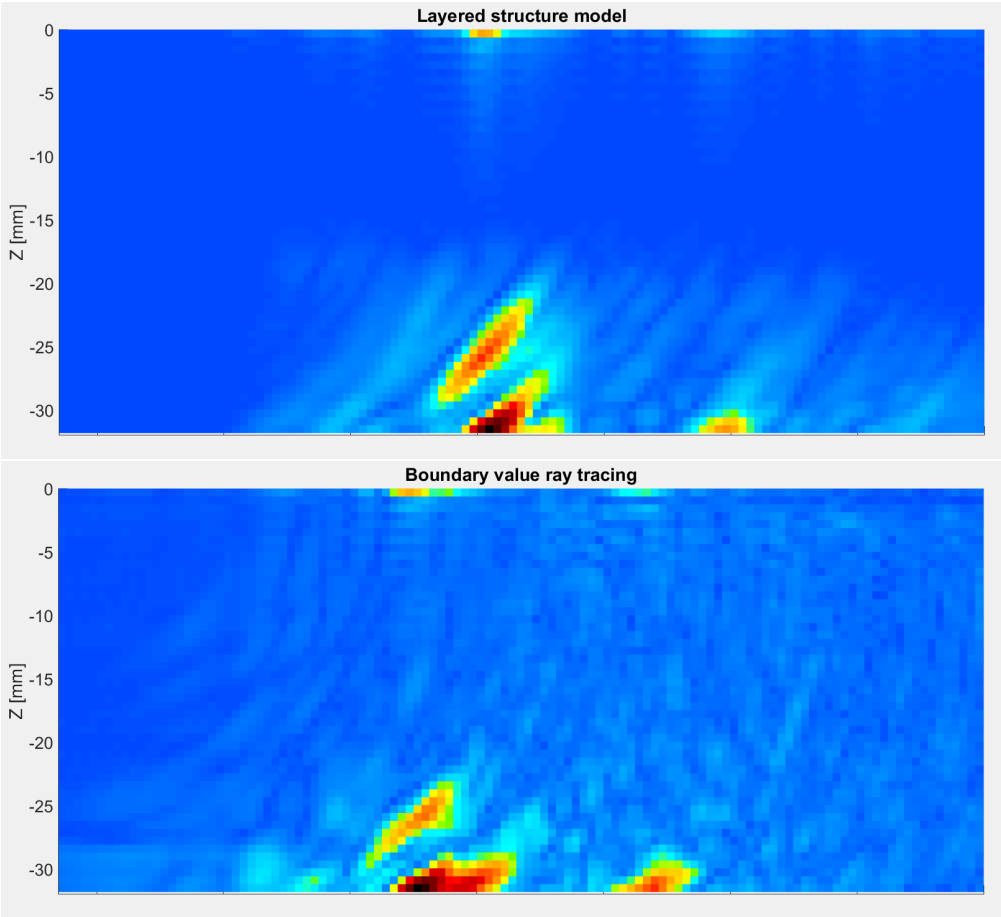

Figure 4: Comparison of SAFT results using and the boundary value problem formulation (top) and a layer model with initial value ray tracing (bottom) for ray tracing.

minimizes the error of the calculated travel times.

Compared to populating the travel time matrix with initial value ray tracing, where only 908 of 4680 cells are hit by a ray and thus have an associated time of flight, using the approach described in this paper allowed to obtain times of flight for 4592 cells. Only for cells close to the top surface $z = 0$, no rays could be found, mostly due to total reflection of the ray at the perspex and buffer interfaces. On average, five Newton iterations were required per cell, with a computation time of 1.28 s per Newton iteration on an AMD Opteron 2.8 GHz, i.e. 0.0023 s per ray (as 7 + 49 initial value problems have to be solved, 7 for the ray itself, 49 for the derivatives). As is to be expected, initial value ray tracing is computationally slightly cheaper, with 4.5 s per populated cell. The computation time for boundary value ray tracing can further be reduced using the adaptive strategy outlined above.

Another difference of both approaches is the coverage of the reconstruction plane. Here, the signals in depths above −15 mm contain no information, since the sound cones of the measurement did not reach this area. By matching the modeling to the measurement parameter, the calculation time can be reduced further.

References

[1] K.J. Langenberg, R. Hannemann, T. Kaczorowski, R. Marklein, B. Koehler, C. Schurig, F. Walte. Application of modeling techniques for ultrasonic weld inspection. NDT&E International 33:465-480, 2000.

[2] Analytical methods for modeling of ultrasonic nondestructive testing of anisotropic media. Ultrasonics 42:213-219, 2004.

[3] A. Shlivinsky, K.J. Langenberg. Defect imaging with elastic waves in inhomogeneous-anisotropic materials with composite geometries. Ultrasonics 46:89-104, 2007.

[4] M. Kröning, A. Bulavinov, K.M. Reddy, F. Walte, M. Dalichow. Improving the inspectability of stainless-steel and dissimilar metal welded joints using inverse phase-matching of phased array time-domain signals. Proceedings of the 17th WCNDT, Shanghai, paper 451, 2008.

[5] S. Prudikov, A. Bulavinov, R. Pinchuk. Innovative ultrasonic testing (UT) of nuclear components by sampling phased array with 3D visualization of inspection results. DGZfP Proceedings BB 125, paper Th.2.C.6, 2010.

[6] C. Höhne, S. Kolkoori, M.U. Rahman, R. Boehm, J. Prager. SAFT imaging of transverse cracks in asutenitic and dissimilar welds. J. Nondestruct. Eval. 32(1):51-66, 2013.

[7] K. Matthies et al., Ultraschallprüfung von austenitischen Werkstoffen. DVS Media GmbH, Berlin, 2009.

[8] K.J. Langenberg, R. Marklein, K. Mayer. Theoretische Grundlagen der zerstörungsfreien Materialprüfung mit Ultraschall. Oldenburg Wissenschaftsverlag, München, 2009.

[9] B.R. Julian, D. Gubbins. Three-Dimensional Seismic Ray Tracing. J. Geophys. 43:95-113, 1977.

[10] H. Le Meur, J. Virieux, P. Podvin. Seismic tomography of the Gulf of Corinth: a comparison of methods. Ann. Geofis. 40(1):1-24, 1997.

[11] V. Cerveny. Seismic Ray Theory. Cambridge University Press, 2005.

[12] S.I. Rokhlin, T.K. Bolland, L. Adler. Reflection and refraction of elastic waves on a plane interface between two generally anisotropic media. J. Acoust. Soc. Am. 79(4):906-918, 1986.

[13] P. Deuflhard, F. Bornemann. Scientific Computing with Ordinary Differential Equations. Springer, 2002

[14] P. Deuflhard. Newton Methods for Nonlinear Problems. Affine Invariance and Adaptive Algorithms. Springer, 2006.

[15] J.A. Ogilvy. Computerized ultrasonic ray tracing in austenitic steel. NDT International 18(2):67-77, 1985.

[16] M. Spies, H. Rieder. Sythetic aperture focusing of ultrasonic inspection data to enhance the probability of detection in strongly attenuating materials. NDT&E International 43:425-431, 2010.

[17] W. Müller, V. Schmitz, G. Schäfer. Reconstruction by the synthetic aperture focusing technique (SAFT). Nuclear Engineering and Design 94:393-404, 1986.